

Anisotropic flow and flow fluctuations for Au + Au at $\sqrt{s_{NN}} = 200$ GeV in a multiphase transport model

L. Ma,^{1,2} G. L. Ma,¹ and Y. G. Ma^{1,3,*}

¹*Shanghai Institute of Applied Physics, Chinese Academy of Sciences, Shanghai 201800, China*

²*University of Chinese Academy of Sciences, Beijing 100049, China*

³*Shanghai Tech University, Shanghai 200031, China*

(Dated: July 16, 2018)

Anisotropic flow coefficients and their fluctuations are investigated for Au+Au collisions at center of mass energy $\sqrt{s_{NN}} = 200$ GeV by using a multi-phase transport model with string melting scenario. Experimental results of azimuthal anisotropies by means of the two- and four-particle cumulants are generally well reproduced by the model including both parton cascade and hadronic rescatterings. Event-by-event treatments of the harmonic flow coefficients v_n (for $n = 2, 3$ and 4) are performed, in which event distributions of v_n for different orders are consistent with Gaussian shapes over all centrality bins. Systematic studies on centrality, transverse momentum (p_T) and pseudo-rapidity (η) dependencies of anisotropic flows and quantitative estimations of the flow fluctuations are presented. The p_T and η dependencies of absolute fluctuations for both v_2 and v_3 follow similar trends as their flow coefficients. Relative fluctuation of triangular flow v_3 is slightly centrality-dependent, which is quite different from that of elliptic flow v_2 . It is observed that parton cascade has a large effect on the flow fluctuations, but hadronic scatterings make little contribution to the flow fluctuations, which indicates flow fluctuations are mainly modified during partonic evolution stage.

PACS numbers: 25.75.Nq, 25.75.Ld, 25.75.Gz

I. INTRODUCTION

An extreme hot and dense source composed of deconfined quarks and gluons (Quark Gluon Plasma) is believed to be created in high-energy heavy-ion collision [1]. Because the pressure gradient of source is large enough to translate an initial coordinate space asymmetry to a final momentum space anisotropy, it can be experimentally measured as anisotropic flow. Anisotropic flow, as a typical collective behavior of particles emission, has been proved as a good probe to study the formed source because it can provide important information about equation of state and transport properties of the formed matter in high-energy heavy-ion collisions [2–7]. One of the most striking experimental results ever obtained at Relativistic Heavy Ion Collider (RHIC) is strong elliptic flow (i.e. v_2), which is defined as the second harmonic coefficient of the Fourier expansion of the azimuthal distribution of the final-state particles [8–11]. The averaged magnitude of elliptic flow has been extensively studied as functions of centrality, transverse momentum (p_T), pseudo-rapidity (η), particle type as well as energy and collision systems [12–17]. Since hydrodynamical models have given many comparable descriptions on the measured flow [18–22], it indicates that the hot and dense source is a nearly perfect fluid in the early period of high-energy heavy-ion collisions [1, 2].

In recent years, higher orders of harmonic coefficients in the Fourier expansion of azimuthal distribution (i.e.

v_n for $n = 3, 4, 5\dots$) have attracted much more attention since they are expected to be more sensitive to the properties of Quark Gluon Plasma and equation of state. The higher even orders of harmonic coefficients, e.g. v_4 and v_6 , were systematically studied experimentally, which provide very useful information about the collision dynamics and the properties of the hot dense matter in the initial stage [23]. For higher odd orders of harmonic coefficients, they were ever supposed to vanish due to the source symmetry. However, the importance of fluctuations was realized that the initial fluctuations of geometry asymmetries will be transferred into the final momentum space as the system expands, which finally lead to non-zero values of the odd harmonic flow coefficients [24–26]. It was found that odd orders of harmonic flows are sensitive to not only initial condition but also shear viscosity over entropy density η/s during QGP evolution stage. The studies of the odd orders of harmonic flows, especially third flow harmonic (v_3), are thus of great interests in recent years. For instance, it has been suggested that the third harmonic flow v_3 is responsible for the ridge and shoulder structures in di-hadron azimuthal correlations [27–34]. It was also found that v_3 shows its sensitivity to viscosity and initial state granularity, based on event-by-event relativistic viscous hydrodynamic simulations [35–37].

The measurements of anisotropic flow fluctuations are believed to be a good access to the initial conditions, especially for its fluctuating or correlating properties. The measurements of elliptic flow fluctuation and even higher harmonic flow fluctuations on the event-by-event basis may elucidate both the system dynamics and new phenomena which occur in the early stage of collisions [38–

*Corresponding author. Email: ygma@sinap.ac.cn

40]. The centrality and system-size dependencies of the event-by-event elliptic flow fluctuations in Au+Au collisions at $\sqrt{s_{NN}} = 200$ GeV have been studied by the PHOBOS and the STAR experiments [41–43], which show a relative large fluctuation of 40% in mid-central region. The elliptic flow fluctuations are also theoretically studied with some models including initial state fluctuations [44–46], which disclose the correlations between final flow and the initial geometry fluctuations, as well as some information about the viscosity and other properties of the hot matter created in high-energy heavy-ion collisions.

In this paper, we present a systematic study on harmonic flows and their fluctuations with a multi-phase transport (AMPT) model. The pseudo-rapidity and transverse momentum dependencies have been systematically studied, which provide a better understanding of the source fluctuation properties. The paper is organized as follows: In Sec. II, A multi-phase transport model is briefly introduced. The results and discussions are presented in Sec. III. In Sec. IV, a brief summary is presented.

II. BRIEF DESCRIPTION OF AMPT MODEL

A multi-phase transport model [47] is a useful Monte Carlo model to investigate evolution dynamics for high-energy heavy-ion collisions. Currently, the AMPT model has two versions, i.e. the default version and string-melting version. Both of them consist of four main dynamical components: initial condition, parton cascade, hadronization, and hadronic rescatterings.

For the initial condition, the phase space distributions of minijet partons and soft string excitations are included, which are obtained from the Heavy-Ion Jet Interaction Generator model (HIJING) [48] in which the Glauber model with multiple nucleon scatterings is basically used to describe the initial state of heavy-ion collisions. The multiple scatterings lead to the fluctuations in local energy density or hot spots from both soft and hard interactions which are proportional to local transverse density of participant nucleons. In the string-melting version, both excited strings and minijet partons are melt into partons. However all partons only consist of minijet partons in the default version. Scatterings among partons are then treated according to Zhang’s Parton Cascade (ZPC) model [49] which includes only two-body elastic scatterings with a cross section obtained by the following equation,

$$\frac{d\sigma}{dt} = \frac{9\pi\alpha_s^2}{2} \left(1 + \frac{\mu^2}{s}\right) \frac{1}{(t - \mu^2)^2}, \quad (1)$$

where $\alpha_s = 0.47$ is the strong coupling constant, s and t are the usual Mandelstam variables and μ is the screening mass. When all partons stop interacting with each other, a simple quark coalescence model is used to combine partons into hadrons for the string-melting version.

However, the Lund fragmentation is implemented for the hadronization in the default version. Thus partonic matter is then turned into hadronic matter and the hadronic interactions are subsequently simulated by using A Relativistic Transport (ART) model which includes both elastic and inelastic scatterings for baryon-baryon, baryon-meson and meson-meson interactions [50].

For some collective phenomena in high-energy heavy-ion collisions, it is found that the string-melting version is much more appropriate than the default version with the help of a large parton interaction cross section [23, 47, 51–53]. Therefore, we choose the version of AMPT model with string-melting mechanism with the parton cross section of 10 mb or 3 mb to simulate Au+Au collisions at 200 GeV in this work. We focus on the partonic and hadronic effects on flow and flow fluctuation. For this analysis, we divide the AMPT events into different centrality bins, as described in Table I, where the mean values of participant nucleons $\langle N_P \rangle$ and corresponding impact parameter ranges for each centrality bin are shown. Before we present further results, we should mention that in most calculation results which are shown in this work except Figure 7, 10 mb parton cross section was always used.

TABLE I: The mean values of participant nucleons $\langle N_P \rangle$ and impact parameter intervals corresponding to different centrality bins for Au+Au collisions at 200 GeV in this work.

Centrality	Impact parameter (fm)	$\langle N_P \rangle$
0% - 10%	0.00 - 4.42	345.85±0.10
10% - 20%	4.42 - 6.25	263.45±0.10
20% - 30%	6.25 - 7.65	198.20±0.05
30% - 40%	7.65 - 8.83	146.85±0.10
40% - 50%	8.83 - 9.88	106.10±0.08
50% - 60%	9.88 - 10.82	73.80±0.10
60% - 70%	10.82 - 11.68	48.80±0.10
70% - 80%	11.68 - 12.50	30.60±0.03

III. RESULTS AND DISCUSSION

A. Anisotropic flow coefficients v_n and v_n fluctuations

The collectivity in high-energy heavy-ion collisions can be measured through final particle azimuthal anisotropy [18]. The anisotropy coefficients are generally obtained from Fourier expansion of final particle azimuthal distribution [19, 54], i.e.

$$E \frac{d^3 N}{d^3 p} = \frac{1}{2\pi} \frac{d^2 N}{p_T dp_T dy} \left(1 + \sum_{i=1}^N 2v_n \cos[n(\phi - \psi_{RP})]\right), \quad (2)$$

where E is the energy of the produced particle, p_T is the transverse momentum, y is the rapidity, ϕ represents the azimuthal angle of particle and ψ_{RP} is the reaction plane angle. The Fourier coefficients v_n ($n=1,2,3,\dots$) are

typically used to characterize the different orders of azimuthal anisotropies with the form

$$v_n = \langle \cos(n[\phi - \psi_{RP}]) \rangle, \quad (3)$$

where the bracket $\langle \rangle$ denotes statistical averaging over particles and events. In the AMPT model, reaction plane angle ψ_{RP} is assigned to be zero and the flow harmonic coefficients can be written as $v_n = \langle \cos(n\phi) \rangle$ (for $n=1, 2, 3$). Harmonic flow v_n can also be calculated with respect to the participant plane angle $\psi_n \{P\}$ under participant coordinate system [55] instead of reaction plane angle ψ_{RP} . The participant plane is defined by the principal axis of the participant zone in the following equation

$$\psi_n \{P\} = \frac{1}{n} \left[\arctan \frac{\langle r^n \sin(n\varphi) \rangle}{\langle r^n \cos(n\varphi) \rangle} + \pi \right], \quad (4)$$

where n denotes the n th-order participant plane, r and φ are the coordinate position and azimuthal angle of each parton in AMPT initial state and the average $\langle \dots \rangle$ denotes density weighting. Harmonic flow coefficients with respect to participant plane are defined as

$$v_n \{P\} = \langle \cos[n(\phi - \psi_n \{P\})] \rangle. \quad (5)$$

The above method for the calculation of v_n is referred to as participant plane method which has been popularly used for flow calculations in different models [56]. Because the participant plane angle defines the azimuthal angle of the plane by constructing initial energy distribution in coordinate space, $v_n \{P\}$ with event-by-event fluctuation effects included is more reasonable to compare with experimental data. In Figure 1, we show the event-by-event distributions of $v_n \{P\}$ ($n=2,3,4$) for all charged particles within mid-rapidity for four different centrality bins in Au+Au collisions at 200 GeV, where solid curves are Gaussian fittings. The $v_n \{P\}$ ($n=2,3,4$) distributions are consistent with Gaussian shapes for all the orders and all the centrality bins from the AMPT simulations.

Several methods and techniques have been developed to estimate the flow coefficients experimentally [54, 57–59], such as the event plane method that is reconstructed within mid-rapidity [54] and FTPC event plane method that uses forward- or backward- going tracks in the large rapidity window to determine the event plane. These methods have been widely used in experimental analysis of flow, though it is still argued for them to have some disadvantages [60, 61]. On the other hand, multi-particle correlation method (or cumulant method) has successfully quantified the harmonic flow coefficients, without requiring the reaction or participant plane [10, 58, 62–64]. The contribution of non-flow correlations from lower order correlations can be effectively removed with multi-particle correlation. The cumulant method is expected to partially eliminate detector effects, because it is insensitive to detector acceptance.

A Q-cumulant or direct cumulant method, which calculates cumulants without using multiple loops over tracks and generating functions, has been developed for flow analysis [59]. The Q-cumulant method calculates flow coefficients v_n ($n=2,3,4..$) directly from particle correlations with a flow vector defined as

$$Q_n = \sum_{i=1}^M e^{in\phi_i}, \quad (6)$$

where M is the number of particles.

The cumulants are weighted by averaging over events, which can be expressed in terms of the moments of the magnitude of the corresponding flow vector,

$$\langle\langle 2 \rangle\rangle = \langle\langle e^{in(\phi_1 - \phi_2)} \rangle\rangle = \frac{\sum_{events} (W_2)_i \langle 2 \rangle_i}{\sum_{events} (W_2)_i}, \quad (7)$$

$$\langle\langle 4 \rangle\rangle = \langle\langle e^{in(\phi_1 + \phi_2 - \phi_3 - \phi_4)} \rangle\rangle = \frac{\sum_{events} (W_4)_i \langle 4 \rangle_i}{\sum_{events} (W_4)_i},$$

where the double brackets denote weighted first over the particles and then over the events for two- and four-particle correlations. The weights are the total number of combinations of two- or four-particle correlations, i.e.

$$W_2 = M(M-1), W_4 = M(M-1)(M-2)(M-3), \quad (8)$$

which are used to minimize the effects from multiplicity fluctuations [65].

The final two- and four-particle cumulants can be written as

$$\begin{aligned} C_n \{2\} &= \langle\langle 2 \rangle\rangle, \\ C_n \{4\} &= \langle\langle 4 \rangle\rangle - 2\langle\langle 2 \rangle\rangle^2. \end{aligned} \quad (9)$$

For integral (or reference) flow coefficients, they can be estimated directly from two- and four-particle cumulants by the following equations,

$$v_n \{2\} = \sqrt{C_n \{2\}}, \quad (10)$$

$$v_n \{4\} = \sqrt[4]{-C_n \{4\}}. \quad (11)$$

One can also proceed the calculations of differential flow with a new definition of vectors with particles of interest (POI) and reference particle (REP). For particles labeled as POI, we define a vector

$$p_n = \sum_{i=1}^{m_p} e^{in\psi_i}. \quad (12)$$

For particles labeled as both POI and REP, we define a vector

FIG. 1: (Color online) Distributions of $v_n \{P\}$ [$n=2$ (a), 3 (b), 4 (c)] for different centrality bins in Au+Au collisions at 200 GeV from the AMPT simulations.

$$q_n = \sum_{i=1}^{m_q} e^{in\psi_i}, \quad (13)$$

where m_p and m_q are the number of selected particles. The reduced single-event averaged two- and four-particle correlations can be formalized as $\langle 2' \rangle$ and $\langle 4' \rangle$ [59]. Thus the two- and four-particle differential cumulants are given by,

$$\begin{aligned} d_n \{2\} &= \langle \langle 2' \rangle \rangle, \\ d_n \{4\} &= \langle \langle 4' \rangle \rangle - 2\langle \langle 2' \rangle \rangle \langle \langle 2 \rangle \rangle. \end{aligned} \quad (14)$$

Estimations of differential flow coefficients are expressed as:

$$v'_n \{2\} = \frac{d_n \{2\}}{\sqrt{C_n \{2\}}}, \quad (15)$$

$$v'_n \{4\} = \frac{d_n \{4\}}{-C_n \{4\}^{3/4}}. \quad (16)$$

In addition, it was suggested that if the Gaussian form of flow fluctuations in the participant plane is taken with the definitions of cumulants flow [55], one would have

$$v_n \{2\}^2 = \langle v_n \rangle^2 + \sigma_{v_n}^2 + \delta_n, \quad (17)$$

$$v_n \{4\}^2 = \sqrt{\langle v_n \rangle^4 - 2\langle v_n \rangle^2 \sigma_{v_n}^2 - \sigma_{v_n}^4} \approx \langle v_n \rangle^2 - \sigma_{v_n}^2, \quad (18)$$

where δ_n is the non-flow contribution from correlations not related to the reaction plane, and σ_{v_n} is the absolute flow fluctuation. The approximation in Equation (18) is valid when $\sigma_{v_n} \ll v_n$ and higher order moments are negligible. In above definitions, two-particle cumulant flow contains non-flow contribution, and four-particle cumulant flow is unaffected by non-flow effect but by flow fluctuations [66].

If the distribution of $v_n \{P\}$ is with a Gaussian shape as shown in Figure 1, one can take advantage of difference between Equation (17) and Equation (18) to estimate of the total flow fluctuation in the limit of small fluctuation,

$$\sigma_{v_n}(Q) = \sqrt{\frac{v_n^2 \{2\} - v_n^2 \{4\}}{2}} \approx \sqrt{\sigma_{v_n}^2 + \delta_n/2}, \quad (19)$$

$$R_{v_n}(Q) = \sqrt{\frac{v_n^2 \{2\} - v_n^2 \{4\}}{v_n^2 \{2\} + v_n^2 \{4\}}}, \quad (20)$$

where Equation (19) gives an absolute flow fluctuation estimation and Equation (20) presents a relative flow fluctuation estimation. It should be noted that the flow fluctuations defined with above formulas contain non-flow contributions, therefore they can only be treated as up-limits for both absolute and relative flow fluctuations. The up-limits of elliptic flow v_2 fluctuations with the above definition have been studied both experimentally and theoretically so far [55, 67].

Non-flow correlations do have substantial effects on the measurements of flow fluctuations. Previous studies show that it is difficult to disentangle non-flow effects and flow fluctuations if without other assumptions due to initial geometry fluctuations [55, 68]. A recent work shows that a large pseudo-rapidity gap between particles can effectively reduce short-range non-flow contributions [69]. However, the validity of the large pseudo-rapidity gap assumption can not be unambiguously applicable [39], therefore non-flow is not eliminated completely in this way and additional fluctuations from unknown sources could lead to non-ignorable contribution on the difference between $v_n \{2\}$ and $v_n \{4\}$. However, the quantity $R_{v_n}(Q)$ can be treated as a reasonable approximation of relative flow fluctuation, under the assumption that non-flow only takes a small portion of contribution ($\leq 10\%$).

Since it is still uncertain if one can reliably obtain true flow fluctuations from cumulant measurements, we try a compensative way to do event-by-event treatment on $v_n \{P\}$ based on its standard definition in AMPT model simulations. In this way, the absolute flow fluctuation

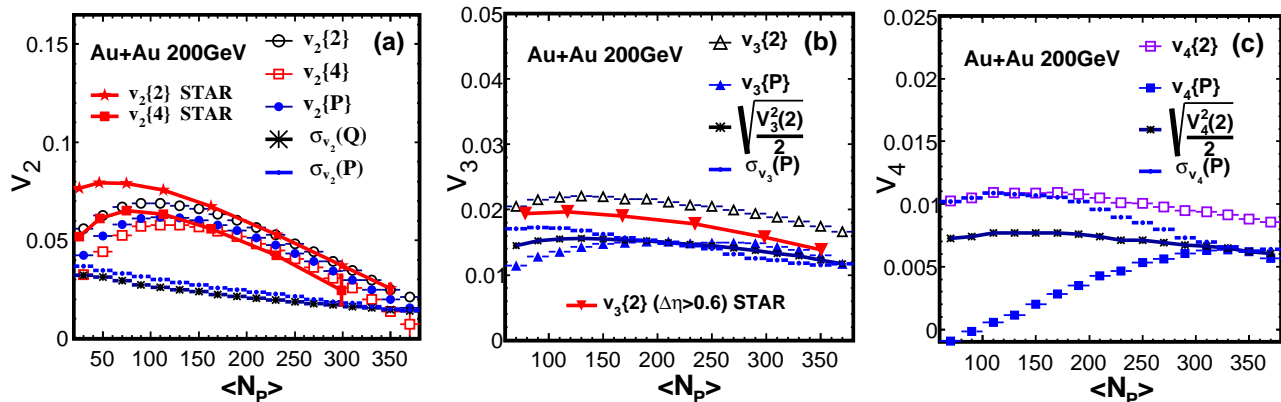


FIG. 2: (Color online) Flow coefficients v_n [$n=2$ (a), 3 (b), 4 (c)] for all charged particles in mid-rapidity ($|\eta| \leq 1.0$) from participant plane method and Q-cumulant method as a function of $\langle N_P \rangle$ in Au+Au collision at 200 GeV. Absolute flow fluctuation $\sigma_{v_n}(Q)$ (black dot line) and $\sigma_{v_n}(P)$ (blue dot line) are also presented, and experimental results from the STAR experiment are shown (red solid star for $v_2\{2\}$ and red solid square for $v_2\{4\}$). Experimental measurement of $v_3\{2\}$ with pseudorapidity gap applied is also shown for comparison (in middle panel) [26].

$\sigma_{v_n}(P)$ and the relative flow fluctuation $R_{v_n}(P)$ can be defined as,

$$\sigma_{v_n}(P) = \sqrt{\langle v_n\{P\}^2 \rangle - \langle v_n\{P\} \rangle^2}, \quad (21)$$

$$R_{v_n}(P) = \sqrt{\frac{\langle v_n\{P\}^2 \rangle - \langle v_n\{P\} \rangle^2}{\langle v_n\{P\} \rangle^2}}, \quad (22)$$

where brackets $\langle \rangle$ denote event averaging. Figure 2 comparatively shows the integrated flow coefficients v_n for charged particles ($|\eta| \leq 1.0$) as a function of $\langle N_P \rangle$ based on Q-cumulant method and participant plane method, as well as the absolute flow fluctuations of $\sigma_{v_n}(Q)$ and $\sigma_{v_n}(P)$ in Au+Au collisions at 200 GeV. The AMPT results for $v_2\{2\}$ and $v_2\{4\}$ are in good agreement with the STAR experimental results [70] from mid-central to central Au+Au collisions. The absolute elliptic flow fluctuations σ_{v_2} monotonously decrease with N_P . The standard deviation of participant flow value $\sigma_{v_2}(P)$ overestimates flow fluctuation $\sigma_{v_2}(Q)$ which contains some additional non-flow effect. It is found that v_2 is dominated by its fluctuation for the most central or the most peripheral Au+Au collisions. For higher order harmonics especially the third harmonic, the fourth power of $v_3\{4\}$ is almost consistent with zero within the error range in the model results which is quite consistent with the recent experiment results [71]. By assuming $v_3\{4\}$ equals to zero, $\sqrt{\frac{v_3^2\{2\}}{2}}$ is presented here instead of the complete form of Equation (19) simply for comparisons. We can see for higher order harmonics v_3 and v_4 , the results from Q-cumulant method show weak centrality dependencies which is similar to the LHC measurements [72]. By comparing $v_3\{P\}$ and $\sigma_{v_3}(P)$, it is clearly seen that triangular flow mainly comes from fluctuation. From the AMPT

calculations, $v_4\{P\}$ shows obvious centrality dependence which falls to almost zero for the most peripheral collisions. $\sigma_{v_4}(P)$ only has the similar magnitude with $v_4\{P\}$ only for the most central events, but with larger $\sigma_{v_4}(P)$ than $v_4\{P\}$ for non-central collisions. For $v_3\{4\}$ and $v_4\{4\}$ not shown here, we found that they are consistent with zero within the errors, which is similar to the STAR preliminary measurements [73].

It was suggested that $v_n\{2\}$ should be likely equal to $v_n\{P\}$ [55]. For this reason, $\sigma_{v_n}(P)$ should be smaller than $\sigma_{v_n}(Q)$ under positive non-flow assumption, as the difference between $\sigma_{v_n}(P)$ and $\sigma_{v_n}(Q)$ is totally caused by non-flow effect. But as shown in Figure 2, $\sigma_{v_n}(P)$ is slightly larger than $\sigma_{v_n}(Q)$ over all the centrality ranges which indicates that $\sigma_{v_n}(Q)$ is not exactly the standard deviation of $v_n\{P\}$ defined by $\sigma_{v_n}(P)$. However, it does little effect if we only make magnitude estimate of flow fluctuation and study the trends of flow coefficients and their fluctuations. Nevertheless, $\sigma_{v_2}(P)$ can give general estimation of v_2 fluctuations in magnitude, and $\sigma_{v_n}(P)$ can be used to study the fluctuations of higher harmonic coefficients in the similar way.

B. v_n fluctuations as functions of transverse momentum and pseudo-rapidity

It is also important to study the transverse momentum (p_T) dependence of anisotropic flow from cumulant method and make comparisons with the results from participant plane method. Figure 3 shows the differential v_2 and v_3 obtained with the Q-cumulant method and participant plane method, in comparison with two-particle $v_2\{2\}$ and four-particle $v_2\{4\}$ from the RHIC experiments [74, 75]. It is observed that the AMPT results of $v_2\{4\}$ is consistent with the experimental data, but $v_2\{2\}$ is slightly larger than the experimental data. Ab-

solute flow fluctuations of $\sigma_{v_2}(Q)$ and $\sigma_{v_3}(P)$ are also shown. It is found that absolute v_2 fluctuation shows similar transverse momentum and centrality dependencies as v_2 . For the most central Au+Au collisions (0-10%), v_2 is mainly dominated by its absolute fluctuation. On the other hand, v_3 has very weak centrality dependence, which differs significantly from that of v_2 . It is clearly seen that absolute fluctuation of v_3 has a similar magnitude as v_3 , which is consistent with the fact that the origin of triangular flow is due to initial fluctuations.

for charged hadrons on pseudo-rapidity η with both Q-cumulant and participant plane methods with the AMPT model. Figure 4 shows the pseudo-rapidity dependencies of the elliptic flow and triangular flow for six centrality bins in Au+Au collisions at 200 GeV from the AMPT model simulations. $v_2(\eta)$ for all centrality bins are of Gaussian shape, but the magnitude varies with centrality bins. However, the magnitude of triangular flow $v_3(\eta)$ shows weak centrality dependence as that of $v_3(p_T)$. The absolute fluctuations, $\sigma_{v_2}(Q)$ and $\sigma_{v_3}(P)$, show similar trends as their flow coefficients. Triangular flow fluctuation of $\sqrt{v_3^2\{2\}}/2$ from Q-cumulant method are also shown for comparison.

FIG. 3: (Color online) Differential v_2 (Upper six panels) and v_3 (Lower six panels) as a function of transverse momentum for charged particles in mid-rapidity for six centrality bins in Au+Au collision at 200 GeV. $v_2\{2\}$, $v_2\{4\}$ are from Q-cumulant methods, and $v_2\{P\}$ is from participant plane method. Black Dots with grey shadow areas show the magnitudes of absolute flow fluctuation. The open and solid star symbols represents experimental results for two-particle $v_2\{2\}$ and four-particle $v_2\{4\}$ respectively. The absolute v_3 fluctuation from Q-cumulant method $\sqrt{v_3^2\{2\}}/2$ and participant plane method $\sigma_{v_3}(P)$ are represented with grey solid squares and blue dot line separately. Experimental $v_3\{TPC\}$ data (read solid down-triangles) which were based on the TPC event plane method are taken from Ref. [71] for comparison.

As pseudo-rapidity (η) dependence of anisotropic flow gives additional information about the longitudinal expansion of the created medium, we investigate the dependencies of elliptic flows v_2 and triangular flow v_3

FIG. 4: (Color online) The AMPT results on v_2 (upper six panels) and v_3 (lower six panels) from Q-cumulant method and participant plane method as a function of pseudo-rapidity for six centrality bins in Au+Au collisions at 200 GeV. Experimental $v_3\{TPC\}$ data are also taken from Ref. [71].

Transverse momentum dependence of relative flow fluctuation has attracted much attentions in both theoretical and experimental communities [56, 76]. Within

the framework of AMPT model, we investigate both transverse momentum and pseudo-rapidity dependencies of relative flow fluctuations for different centrality bins in Au+Au collisions at 200 GeV. In Figure 5, $R_{v_2}(p_T)$ shows similar trend as seen those in Pb+Pb collisions at LHC energy [76], which suggests that elliptic flow fluctuation may be controlled by a common mechanism between the two energies. R_{v_2} for the most central collisions (0%-10%) shows much larger magnitude than those for other centrality bins over the whole p_T range, which is consistent with the fact that elliptic flow is dominated by its fluctuation in the most central collisions. For R_{v_3} , it has little p_T dependence as R_{v_2} . However, unlike R_{v_2} , R_{v_3} shows a monotonic increasing behavior from central to peripheral collisions, which actually is driven by both centrality dependencies of v_3 and σ_{v_3} together. On the other hand, it indicates the contribution of v_3 fluctuation becomes more significant in more peripheral collisions.

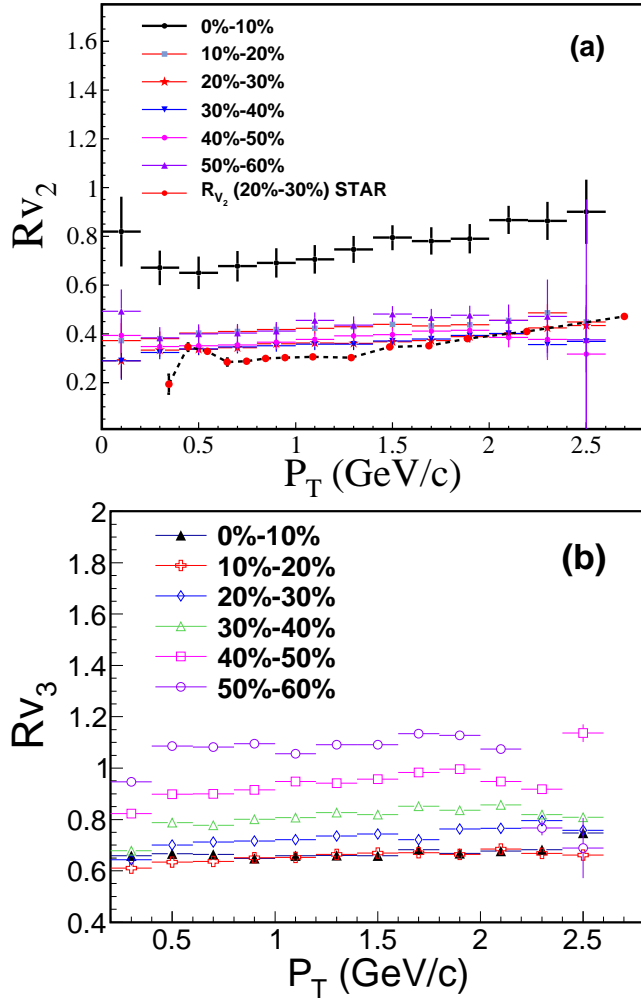


FIG. 5: (Color online) The AMPT results on relative elliptic (upper panel) and triangular (lower panel) flow fluctuations as a function of transverse momentum p_T at different centrality bins in Au+Au collisions at 200 GeV. Experimental v_2 fluctuation data are derived from Ref. [74, 75].

Elliptic flow fluctuation R_{v_2} and triangular flow fluctuation R_{v_3} are presented as a function of pseudo-rapidity η in Figure 6. R_{v_2} for the most central collisions is quite flat over the whole η range, which is different from that for the non-central collisions in which R_{v_2} shows slight η dependence with a wide Gaussian shape. It is interesting that the experimental results of v_2 fluctuation versus η shows little pseudo-rapidity dependence for Pb+Pb collision at 2.76 TeV [77]. On the other hand, R_{v_3} shows no significant η dependence for any centrality bin.

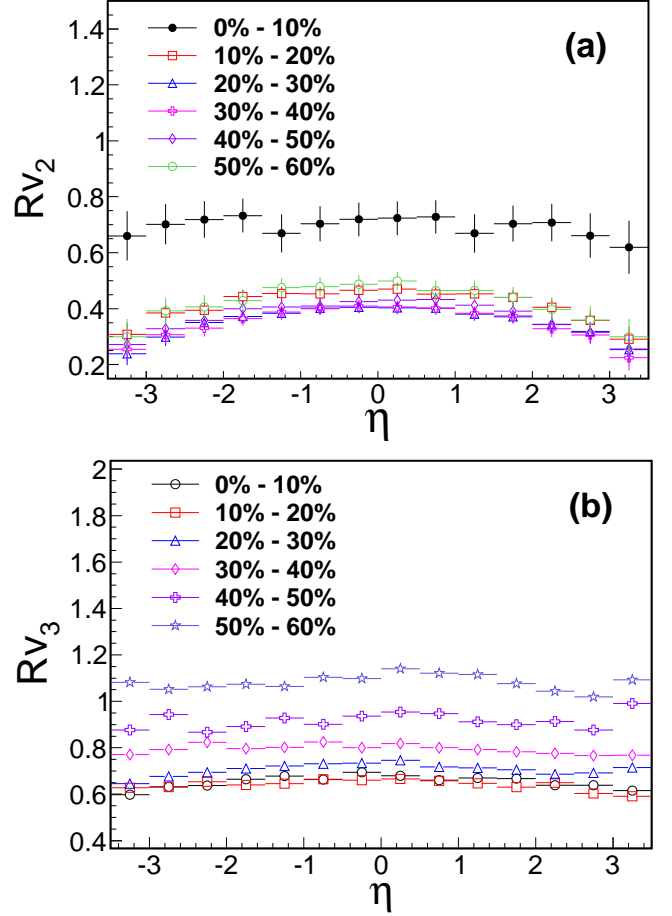


FIG. 6: (Color online) AMPT results on relative elliptic (upper panel) and triangular (lower panel) flow fluctuations as a function of pseudo-rapidity η at different centrality bins in Au+Au collisions at 200 GeV.

C. Initial partonic effect and final hadron scattering effect on flow fluctuations

The parton interaction cross section in the AMPT model has shown a significant effect on final flow coefficients, meanwhile final hadronic rescatterings (FHR) also have considerable influence on the magnitude of the flow coefficients [23]. It is essential to investigate the effects on anisotropy fluctuations from partonic stage and

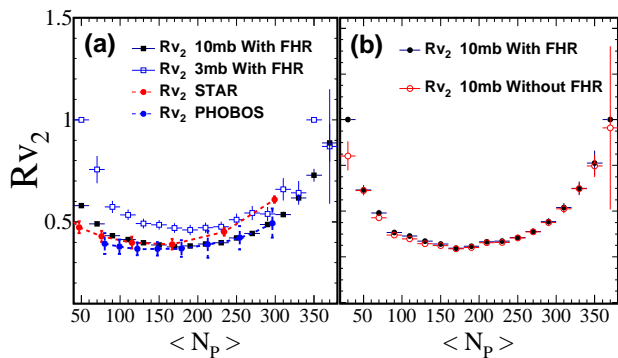


FIG. 7: (Color online) The AMPT results on elliptic flow fluctuation R_{v_2} as a function of $\langle N_P \rangle$ for Au+Au collision at 200 GeV, where panel (a) shows R_{v_2} from AMPT simulations with parton interaction cross section of 3mb and 10mb with final hadronic rescatterings, and panel (b) shows R_{v_2} with and without final hadronic scatterings. Flow fluctuations are compared to STAR and PHOBOS data [39, 40]. The PHOBOS data errors are quoted from Ref. [78].

hadronic stage, since it may shed light on the evolution dynamics of the source in high-energy heavy-ion collisions. Figure 7 shows that relative fluctuations of elliptic flow v_2 as a function of $\langle N_P \rangle$ for charged hadrons in mid-rapidity ($|\eta| \leq 1$) in Au+Au collisions at 200 GeV from AMPT simulations with parton interaction cross section of 3 mb or 10 mb. Relative fluctuation R_{v_2} with parton interaction cross section of 10 mb shows smaller values than that with parton interaction cross section of 3 mb. It indicates that large parton cross section significantly reduces relative flow fluctuation. From the quantitative comparison between the calculations and the data, 10 mb parton cross section seems have better description to the data. Figure 7 (b) gives the comparison of R_{v_2} between with and without final hadronic rescatterings, which suggests that final state hadron rescattering effect essentially makes little effect on relative flow fluctuation.

Since R_{v_2} is not affected by hadron rescattering process, therefore it can reflect the information about strong partonic interactions in the early partonic stage. Experimental measurements on both integral and differential flow fluctuations could serve as prospective constraints on the initial partonic stage for theoretical model simulations.

IV. SUMMARY

In summary, within the framework of a multi-phase transport model, we studied anisotropic flows v_n and their flow fluctuations based on Q-cumulant and participant plane methods for charged particles at mid-rapidity in Au+Au collisions at 200 GeV. With a large parton interaction cross section and final hadronic rescatterings, experimental results of both integral and differential flows with cumulant method are generally well reproduced. Flow fluctuations defined by cumulants and standard deviation from event-by-event treatment show similar trend but slight difference in magnitude. Elliptic flow coefficient v_2 for the most central collisions are dominated by flow fluctuation, but triangular flow v_3 comes from fluctuation for all centrality bins. Flow coefficients and flow fluctuations as functions of transverse momentum and pseudo-rapidity are also investigated, which show that absolute fluctuations for differential v_n ($n=2, 3$) follows the same trend as their flow coefficients. The parton interaction cross section in the AMPT model calculations shows a significant effect on flow fluctuation, which indicate the modifications of flow fluctuations arise during partonic evolution stage.

Acknowledgement: This work was supported in part by the Major State Basic Research Development Program in China under Contract No. 2014CB845400, the National Natural Science Foundation of China under Contract Nos. 11035009, 11220101005, 10979074, 11175232, 11375251 and the Knowledge Innovation Project of Chinese Academy of Sciences under Grant No. KJCX2-EW-N01.

-
- [1] I. Arsene et al. [BRAHMS Collaboration], Nucl. Phys. A **757**, 1 (2005); B. B. Back et al. [PHOBOS Collaboration], Nucl. Phys. A **757**, 28 (2005); J. Adames et al. [STAR Collaboration], Nucl. Phys. A **757**, 102 (2005); S. S. Adler et al. [PHENIX Collaboration], Nucl. Phys. A **757**, 184 (2005).
- [2] P. Romatschke and U. Romatschke, Phys. Rev. Lett. **99**, 172301 (2007) [arXiv:0706.1522 [nucl-th]].
- [3] H. Song and U. W. Heinz, Phys. Rev. C **77**, 064901 (2008) [arXiv:0712.3715 [nucl-th]].
- [4] H. -J. Drescher, A. Dumitru, C. Gombeaud and J. -Y. Ollitrault, Phys. Rev. C **76**, 024905 (2007) [arXiv:0704.3553 [nucl-th]].
- [5] Z. Xu, C. Greiner and H. Stoecker, Phys. Rev. Lett. **101**, 082302 (2008) [arXiv:0711.0961 [nucl-th]].
- [6] V. Greco, M. Colonna, M. Di Toro and G. Ferini, [arXiv:0811.3170 [hep-ph]].
- [7] M. Luzum and P. Romatschke, Phys. Rev. C **78**, 034915 (2008) [Erratum-ibid. C **79**, 039903 (2009)] [arXiv:0804.4015 [nucl-th]].
- [8] K. H. Ackermann et al. [STAR Collaboration], Phys. Rev. Lett. **86**, 402 (2001) [nucl-ex/0009011].
- [9] C. Adler et al. [STAR Collaboration], Phys. Rev. Lett. **87**, 182301 (2001) [nucl-ex/0107003].
- [10] K. Adcox et al. [PHENIX Collaboration], Phys. Rev. Lett. **89**, 212301 (2002) [nucl-ex/0204005].
- [11] B. B. Back et al. [PHOBOS Collaboration], Phys. Rev. Lett. **89**, 222301 (2002) [nucl-ex/0205021].
- [12] J. Adams et al. [STAR Collaboration], Phys. Rev. Lett. **92**, 052302 (2004) [nucl-ex/0306007].

- [13] B. B. Back *et al.* [PHOBOS Collaboration], Phys. Rev. Lett. **94**, 122303 (2005) [nucl-ex/0406021].
- [14] L. Adamczyk *et al.* [STAR Collaboration], Phys. Rev. C **88**, 014902 (2013).
- [15] L. Kumar, Nucl. Phys. A 904-905, 256c (2013).
- [16] J. Tian, J. H. Chen, Y. G. Ma *et al.*, Phys. Rev. C **79**, 067901 (2009).
- [17] C. M. Ko *et al.*, Nucl. Sci. Tech. **24**, 050525 (2013) ; J. Xu, Taesoo Song, Che Ming Ko, and Feng Li, Phys. Rev. Lett. **112**, 012301 (2014) .
- [18] J. -Y. Ollitrault, Phys. Rev. D **46**, 229 (1992).
- [19] S. Voloshin and Y. Zhang, Z. Phys. C **70**, 665 (1996) [hep-ph/9407282].
- [20] P. F. Kolb, J. Sollfrank and U. W. Heinz, Phys. Lett. B **459**, 667 (1999) [nucl-th/9906003].
- [21] U. W. Heinz, J. Phys. G **31**, S717 (2005) [nucl-th/0412094].
- [22] P. Kovtun, D. T. Son and A. O. Starinets, Phys. Rev. Lett. **94**, 111601 (2005) [hep-th/0405231].
- [23] L. -W. Chen, C. M. Ko and Z. -W. Lin, Phys. Rev. C **69**, 031901 (2004) [nucl-th/0312124].
- [24] B. Alver and G. Roland, Phys. Rev. C **81**, 054905 (2010) [Erratum-ibid. C **82**, 039903 (2010)] [arXiv:1003.0194 [nucl-th]].
- [25] G. -L. Ma and X. -N. Wang, Phys. Rev. Lett. **106**, 162301 (2011) [arXiv:1011.5249 [nucl-th]].
- [26] S. Gavin and G. Moschelli, Phys. Rev. C **86**, 034902 (2012).
- [27] J. Adams *et al.* [STAR Collaboration], Phys. Rev. Lett. **95**, 152301 (2005) [nucl-ex/0501016].
- [28] F. Wang [STAR Collaboration], J. Phys. G **30**, S1299 (2004) [nucl-ex/0404010]; F. Q. Wang, Prog. Part. Nucl. Phys. **74**, 35 (2014).
- [29] J. Putschke, J. Phys. G **34**, S679 (2007) [nucl-ex/0701074 [nucl-ex]].
- [30] J. Adams *et al.* [Star Collaboration], Phys. Rev. C **75**, 034901 (2007) [nucl-ex/0607003].
- [31] J. Xu and C. M. Ko, Phys. Rev. C **83**, 021903 (2011) [arXiv:1011.3750 [nucl-th]].
- [32] P. Sorensen, arXiv:0808.0503 [nucl-ex].
- [33] Y. H. Zhu, Y. G. Ma, J. H. Chen, G. L. Ma, S. Zhang, C. Zhong, Phys. Rev. C **87**, 024904 (2013).
- [34] L. Yi, F. Q. Wang, A. H. Tang, J. Phys. G **40**, 035111 (2013).
- [35] B. Schenke, S. Jeon and C. Gale, Phys. Rev. C **85**, 024901 (2012) [arXiv:1109.6289 [hep-ph]].
- [36] B. Schenke, S. Jeon and C. Gale, Phys. Rev. C **82**, 014903 (2010) [arXiv:1004.1408 [hep-ph]].
- [37] B. Schenke, S. Jeon and C. Gale, Phys. Rev. Lett. **106**, 042301 (2011) [arXiv:1009.3244 [hep-ph]].
- [38] H. -J. Drescher and Y. Nara, Phys. Rev. C **76**, 041903 (2007) [arXiv:0707.0249 [nucl-th]].
- [39] B. Alver *et al.* [PHOBOS Collaboration], Phys. Rev. Lett. **104**, 142301 (2010) [nucl-ex/0702036].
- [40] G. Agakishiev *et al.* [STAR Collaboration], Phys. Rev. C **86**, 014904 (2012) [arXiv:1111.5637 [nucl-ex]].
- [41] P. Sorensen [STAR Collaboration], J. Phys. G **34**, S897 (2007) [nucl-ex/0612021].
- [42] B. Alver *et al.* [PHOBOS Collaboration], Phys. Rev. Lett. **98**, 242302 (2007) [nucl-ex/0610037].
- [43] B. Alver *et al.* [PHOBOS Collaboration], J. Phys. G **34**, S907 (2007) [nucl-ex/0701049].
- [44] R. Andrade, F. Grassi, Y. Hama, T. Kodama and O. Socolowski, Jr., Phys. Rev. Lett. **97**, 202302 (2006) [nucl-th/0608067].
- [45] H. Petersen, G. -Y. Qin, S. A. Bass and B. Muller, Phys. Rev. C **82**, 041901 (2010) [arXiv:1008.0625 [nucl-th]].
- [46] L. X. Han, G. L. Ma, Y. G. Ma, X. Z. Cai, J. H. Chen, S. Zhang and C. Zhong, Phys. Rev. C **84**, 064907 (2011) [arXiv:1105.5415 [nucl-th]].
- [47] Z. -W. Lin, C. M. Ko, B. -A. Li, B. Zhang and S. Pal, Phys. Rev. C **72**, 064901 (2005) [nucl-th/0411110].
- [48] X. -N. Wang and M. Gyulassy, Phys. Rev. D **44**, 3501 (1991).
- [49] B. Zhang, Comput. Phys. Commun. **109**, 193 (1998) [arXiv:nucl-th/9709009].
- [50] B. A. Li and C. M. Ko, Phys. Rev. C **52**, 2037 (1995) [arXiv:nucl-th/9505016].
- [51] J. H. Chen, Y. G. Ma, G. L. Ma *et al.*, Phys. Rev. C **74**, 064902 (2006).
- [52] B. Zhang, L. W. Chen and C. M. Ko, Phys. Rev. C **72**, 024906 (2005) [arXiv:nucl-th/0502056].
- [53] G. L. Ma and B. Zhang, Phys. Lett. B **700**, 39 (2011) [arXiv:1101.1701 [nucl-th]].
- [54] A. M. Poskanzer and S. A. Voloshin, Phys. Rev. C **58**, 1671 (1998) [nucl-ex/9805001].
- [55] S. A. Voloshin, A. M. Poskanzer, A. Tang and G. Wang, Phys. Lett. B **659**, 537 (2008) [arXiv:0708.0800 [nucl-th]].
- [56] R. Derradi de Souza, J. Takahashi, T. Kodama and P. Sorensen, Phys. Rev. C **85**, 054909 (2012) [arXiv:1110.5698 [hep-ph]].
- [57] S. A. Voloshin, A. M. Poskanzer and R. Snellings, arXiv:0809.2949 [nucl-ex].
- [58] N. Borghini, P. M. Dinh and J. -Y. Ollitrault, Phys. Rev. C **64**, 054901 (2001) [nucl-th/0105040].
- [59] A. Bilandzic, R. Snellings and S. Voloshin, Phys. Rev. C **83**, 044913 (2011) [arXiv:1010.0233 [nucl-ex]].
- [60] M. Luzum and J. -Y. Ollitrault, Phys. Rev. C **87**, 044907 (2013) [arXiv:1209.2323 [nucl-ex]].
- [61] K. Xiao, F. Liu and F. Wang, Phys. Rev. C **87**, 011901 (2013) [arXiv:1208.1195 [nucl-th]].
- [62] N. Borghini, P. M. Dinh and J. -Y. Ollitrault, Phys. Rev. C **63**, 054906 (2001) [nucl-th/0007063].
- [63] C. Adler *et al.* [STAR Collaboration], Phys. Rev. C **66**, 034904 (2002) [nucl-ex/0206001].
- [64] J. Wang, Y. G. Ma, G. Q. Zhang *et al.*, Nucl. Sci. Tech. **24**, 030501 (2013).
- [65] A. Bilandzic, PhD. thesis, Nikhef and Utrecht University, 2011.
- [66] R. S. Bhalerao and J. -Y. Ollitrault, Phys. Lett. B **641**, 260 (2006) [nucl-th/0607009].
- [67] P. Sorensen, arXiv:0905.0174 [nucl-ex].
- [68] J. -Y. Ollitrault, A. M. Poskanzer and S. A. Voloshin, Phys. Rev. C **80**, 014904 (2009) [arXiv:0904.2315 [nucl-ex]].
- [69] L. Xu, L. Yi, D. Kikola, J. Konzer, F. Wang and W. Xie, Phys. Rev. C **86**, 024910 (2012) [arXiv:1204.2815 [nucl-ex]].
- [70] J. Adams *et al.* [STAR Collaboration], Phys. Rev. C **72**, 014904 (2005) [nucl-ex/0409033].
- [71] L. Adamczyk *et al.* [STAR Collaboration], Phys. Rev. C **88**, 014904 (2013) [arXiv:1301.2187 [nucl-ex]].
- [72] K. Aamodt *et al.* [ALICE Collaboration], Phys. Rev. Lett. **107**, 032301 (2011) [arXiv:1105.3865 [nucl-ex]].
- [73] P. Sorensen [STAR Collaboration], J. Phys. G **38**, 124029 (2011) [arXiv:1110.0737 [nucl-ex]].
- [74] S. Afanasiev *et al.* [PHENIX Collaboration], Phys. Rev. C **80**, 024909 (2009) [arXiv:0905.1070 [nucl-ex]].

- [75] R. Snellings, *New J. Phys.* **13**, 055008 (2011) [arXiv:1102.3010 [nucl-ex]].
- [76] B. Abelev *et al.* [ALICE Collaboration], *Phys. Lett. B* **719**, 18 (2013) [arXiv:1205.5761 [nucl-ex]].
- [77] A. Hansen [ALICE Collaboration], [arXiv:1210.7095 [nucl-ex]].
- [78] B. Alver *et al.* [The PHOBOS Collaboration], *Phys. Rev. C* **81**, 034915 (2008) [arXiv:1002.0534 [nucl-ex]].

